Journal of the Korean Institute of Navigation
Pusan Korea, Vol. 25. No. 4., pp. 471~476, 2001

A Study on Ocean Waves with Free Surface around the Moving Underwater Vehicle

*Seung-Hyun Kwag**

항해중인 잠수정 주위의 자유표면 해양파 연구

곽 승 현*

〈Contents〉

요 약

항해중인 잠수정 주위의 해양파를 재연하기 위하여 3차원 비압축성 나비에-스톡스 코드가 사용되었다. 수치적으로는 3차미분 풍상차분이 근간을 이룬다. 대양에서 항해 중인 선박에 적용을 하기 위해 프루드 수를 0.4에서 0.7까지로 하였다. 조파저항, 양력, 모우멘트, 압력분포가 재연되었고 이것은 조선소의 초기설계에 사용 할 수 있다. Marker & Cell 방법을 기본으로 사각격자 구조를 만들어 해석하였고, 검증을 위하여 기존의 실험 결과와 비교하였다.

I. INTRODUCTION

Ocean waves around a body of revolution have been formulated and studied in detail. Practically, because of the predominant viscous effect near the boundary layer, the related flow pattern is much more complicated, especially if the body is at an incidence with respect to the flow direction. The wake of the body becomes turbulent, and various types of cross flow separation takes place. The basic hull form of a modern submersible is typically a body of revolution. While maneuvering at high speed, the hull may be subject to severe hydrodynamic forces. Under certain conditions, the moment of forces about the center of buoyance of the body may cause instability. In order to achieve a higher envelope of maneuverability and controllability, the designers of the modern sub-

* 한라대학교 기계공학부 교수

mersible have practical interest in predicting the hydrodynamic response for any given planned movement. Such interest can be best served by parallel efforts in enlarging the data base from controlled laboratory environment and developing accurate computational schemes. Extensive experiments were carried out by various research parties, some of the representative results were borrowed from references; Ramaprian[1] and Intermann[2]. More recently, computational efforts based on newly developed numerical schemes offer encouraging predictions; Vasta[3], Hartwich[4]. This paper represents a study of the accuracy and feasibility of predicting forces and moment on a body of revolution hull form.

Ⅱ. NUMERICAL SCHEME

2.1 Basic equations

Numerical simulations of 3-D free-surface flows are carried out by solving Navier-Stokes equations. The velocity components u, v and w at (n+1) time step are determined by

$$u^{n+1}=(F^n-\Phi_x^n)\triangle t$$
$$v^{n+1}=(G^n-\Phi_y^n)\triangle t \quad \cdots\cdots(1)$$
$$w^{n+1}=(H^n-\Phi_z^n)\triangle t$$

where

$$F^n=\frac{u^n}{\triangle t}+\left(\frac{1}{Re}+\nu_t\right)\nabla^2 u - \left(u^n\frac{\partial u}{\partial x}+v^n\frac{\partial u}{\partial y}+w^n\frac{\partial u}{\partial z}\right) - \frac{\partial}{\partial x}\left\{\nu_t\left(2\frac{\partial u}{\partial x}\right)\right\}-\frac{\partial}{\partial y}\left\{\nu_t\left(\frac{\partial u}{\partial y}+\frac{\partial v}{\partial x}\right)\right\} - \frac{\partial}{\partial z}\left\{\nu_t\left(\frac{\partial u}{\partial z}+\frac{\partial w}{\partial x}\right)\right\}$$

$$G^n=\frac{v^n}{\triangle t}+\left(\frac{1}{Re}+\nu_t\right)\nabla^2 v - \left(u^n\frac{\partial v}{\partial x}+v^n\frac{\partial v}{\partial y}+w^n\frac{\partial v}{\partial z}\right) - \frac{\partial}{\partial x}\left\{\nu_t\left(\frac{\partial u}{\partial y}+\frac{\partial v}{\partial x}\right)\right\}-\frac{\partial}{\partial y}\left\{\nu_t\left(2\frac{\partial v}{\partial y}\right)\right\} - \frac{\partial}{\partial z}\left\{\nu_t\left(\frac{\partial v}{\partial z}+\frac{\partial w}{\partial y}\right)\right\}$$

$$H^n=\frac{w^n}{\triangle t}+\left(\frac{1}{Re}+\nu_t\right)\nabla^2 w - \left(u^n\frac{\partial w}{\partial x}+v^n\frac{\partial w}{\partial y}+w^n\frac{\partial w}{\partial z}\right) - \frac{\partial}{\partial x}\left\{\nu_t\left(\frac{\partial u}{\partial z}+\frac{\partial w}{\partial x}\right)\right\}-\frac{\partial}{\partial y}\left\{\nu_t\left(\frac{\partial v}{\partial z}+\frac{\partial w}{\partial y}\right)\right\} - \frac{\partial}{\partial z}\left\{\nu_t\left(2\frac{\partial w}{\partial z}\right)\right\} \quad \cdots\cdots(2)$$

and

$$\Phi^n=p+\frac{z}{Fn^2} \quad \cdots\cdots(3)$$
$$\nabla^2=\frac{\partial}{\partial x^2}+\frac{\partial}{\partial y^2}+\frac{\partial}{\partial z^2} \quad \cdots\cdots(4)$$

where F_n is Froude number and ν_t is the turbulent eddy viscosity normalized by U_oL.

Differentiating Eq. (1) with respect to x, y and z, we can get

$$\nabla^2\Phi=F_x+G_y+H_z-(u_x^{n+1}+v_y^{n+1}+w_z^{n+1})/\triangle t \quad \cdots\cdots(5)$$

The last term in Eq. (5) is expected to be zero to satisfy the continuity condition. Equation (5) can be solved by the relaxation method.

It is desirable to introduce coordinate transformations which simplify the computational domain in the transformed domain

$$\xi=\xi(x,y,z),\ \eta=\eta(x,y,z),\ \zeta=\zeta(x,y,z) \quad \cdots\cdots(6)$$

Through transformations, Eq. (1) can be written,

$$q_t+Uq_\xi+Vq_\eta+Wq_\zeta=\left(\frac{1}{Re}+\nu_t\right)\nabla^2 q-K-REYSF(\xi,\eta,\zeta) \quad \cdots\cdots(7)$$

where U, V and W are the contravariant velocities, K is the pressure gradient, q is the

velocity vector and *REYSF* is the reynolds stress term. The pressure is calculated by the following relaxation formula,

$$\Phi^{m+1} = \Phi^{m} + \omega \cdot (\Phi^{m+1} - \Phi^{m}) \quad \cdots\cdots (8)$$

where (m+1) denotes the next time step and ω is a relaxation factor.

2.2 Computational procedure and boundary conditions

The N-S and Poisson equations are solved after transformation, in which the calculation proceeds through a sequence of loops each advancing the entire flow configuration through sufficiently small finite time increment. The output of each loop is taken as an initial condition for the next. The computation is performed until the state is steady. An Euler explicit scheme is used for the time marching procedure. Pressures are obtained throughout the fluid domain by solving the Poisson equation. Iterations are automatically stopped when the pressure difference between two consecutive approximations is smaller than a certain quantity ε, chosen a priori.

The third order upstream difference is used for convection terms with the fourth-order truncation error, for example;

$$\begin{aligned} & U \cdot (\delta f/\delta x)_{i,j,k} \\ & = U_{i,j,k} \cdot (f_{i-2,j,k} - 8f_{i-1,j,k} + 8f_{i+1,j,k} - f_{i+2,j,k})/12 \\ & + |U_{i,j,k}| \cdot (f_{i-2,j,k} - 4f_{i-1,j,k} + 6f_{i,j,k} - 4f_{i+1,j,k} + f_{i+2,j,k})/4 \end{aligned} \quad \cdots\cdots (9)$$

As boundary conditions, the following are used.

upstream

$u = 1$, $v = 0$, $w = 0$ and $p = 0$

$\triangle u = \triangle v = \triangle w = 0$

downstream

$u_\xi = v_\xi = w_\xi = 0$

$\triangle u_\xi = \triangle v_\xi = \triangle w_\xi = \triangle p_\xi = 0$

symmetrical

$u_\eta = v_\eta = w_\eta = 0$

$\triangle u_\eta = \triangle v_\eta = \triangle w_\eta = \triangle p_\eta = 0$

body surface

$u = v = w = 0, \quad p_\zeta = 0$

$\triangle u = \triangle v = \triangle w = 0, \quad \triangle p_\zeta = 0$

2.3 Free surface boundary condition

The fluid particle is moved on the free surface by

$$\frac{\partial h}{\partial t} + u\frac{\partial h}{\partial x} - w = 0 \Big|_{z=\zeta} \quad \cdots\cdots (10)$$

The boundary condition for the free surface requires zero tangential stress and a normal stress that balances any externally applied normal stress. The displacement of the particle is given by

$$\triangle x = u \cdot \triangle t, \quad \triangle h = w \cdot \triangle t \quad \cdots\cdots (11)$$

where $\triangle t$ is the time increment. On the other hand, the use of an Euler-type expression of the kinematic free surface boundary condition makes it possible to employ a higher finite difference scheme. The condition can be written as follows:

$$\frac{\partial h_i^{n+1}}{\partial t} + (u_i + \frac{\partial u_i}{\partial z}\triangle h_i) \cdot \frac{\partial h_i^{n+1}}{\partial x} - w_i = 0 \quad \cdots (12)$$

where $h = h(x, t)$ represents the elevation.

Expanding in Taylor series, the derivative term can be discretized by using

$$\frac{\partial h_i^{n+1}}{\partial t} = \frac{1}{2\triangle t} \cdot (h^{n-1} - 4h^{n} + 3h^{n+1}) \quad \cdots\cdots (13)$$

For the $\partial h^{n+1}/\partial x$ derivative, the third order upwind difference(TOUD) is adopted.

$$c\frac{\partial h}{\partial x} = c\frac{1}{6\triangle x}(-2h_{i-3} + 9h_{i-2} - 18h_{i-1} + 11h_i) \quad \cdots\cdots (14)$$

where c is the convective velocity; the right-hand side of eq. (14) can be decomposed into two parts. One is the central differencing term whose mathematical expression can be obtained by suitable Taylor expansions as follows:

$$\frac{c}{24\triangle x}(h_{i-3}-27h_{i-2}+27h_{i-1}-h_i) \quad \cdots\cdots\cdots\cdots (15)$$

The other is the diffusion term, which has the meaning of the fourth derivative of the velocity.

$$\frac{3c}{8\triangle x}(-h_{i-3}+7h_{i-2}-11h_{i-1}+5h_i) \quad \cdots\cdots\cdots\cdots (16)$$

The latter is expected to play a role to compensate the finiteness of the differentiation without phase shift. Here we similarly introduce the third derivative, Eq. (17) which contributes to reduce the phase shift together with damping. It is also obtained by the Taylor expansions around i -1½ as follows:

$$\frac{ac}{(\triangle x)^3}(-h_{i-3}+3h_{i-2}-3h_{i-1}+h_i) \quad \cdots\cdots\cdots\cdots (17)$$

where $a=-\frac{(\triangle x)^2}{6}$ is a constant.

Ⅲ. RESULTS AND DISCUSSION

3.1 Underwater Body of Revolution

The underwater body of revolution was numerically tested at Froude number of 0.4 to 0.7. Fig. 1(a) shows the sectional grid view where the grid size is 104x48x23. Fig. 1(b) is the grid for the revolutional body at incidence. The time increment $\triangle t$ is 0.0005 to meet the Courant condition. The Baldwin-Lomax [5] model is used for the turbulence. Two cases of depth level are taken as a numerical study; d/h=0.16 and 0.245.

For the computation domain, 80% of the vehicle length is occupied in lateral direction, and two and half times in downstream. The grid is made

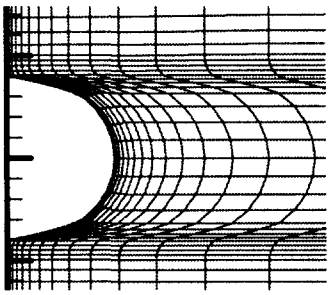

Fig. 1(a). Sectional view of grid generation

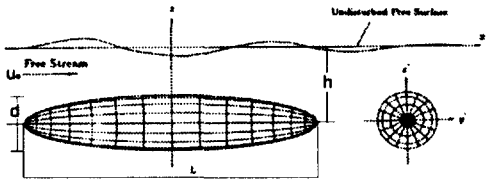

Fig. 1(b). Grid view of revolutional body

as H-H topology to treat the free surface movement more conveniently. The wave height contours are shown in Fig. 2 at two different Froude numbers, where the body length is unity.

In Fig. 3, the velocity vectors can be seen near the bow and near the midship at d/h= 0.16. Fig. 4 shows the comparison of the hydrodynamic coefficients at different Froude numbers. The present

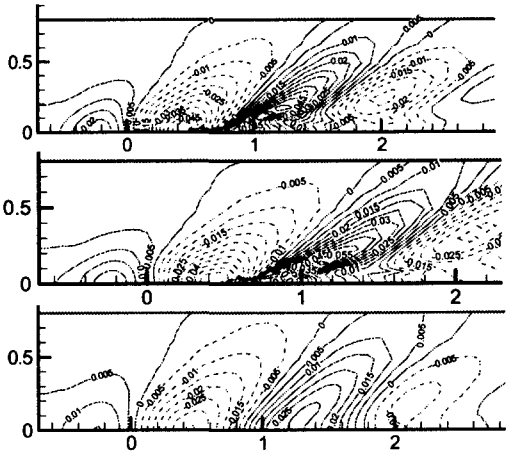

Fig. 2. Free surface waves (*upper: d/h=0.16, t=3.0 middle: d/h=0.16, t=4.0, lower: d/h=0.245, t=3.0*)

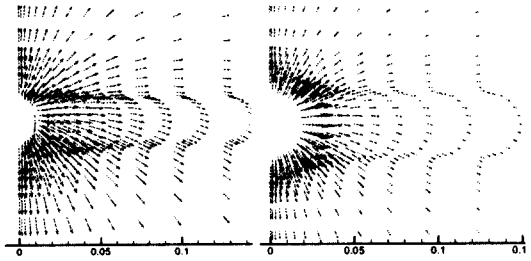

Fig. 3. Velocity vectors at d/h=0.16 (*upper: near the bow, lower: midship*)

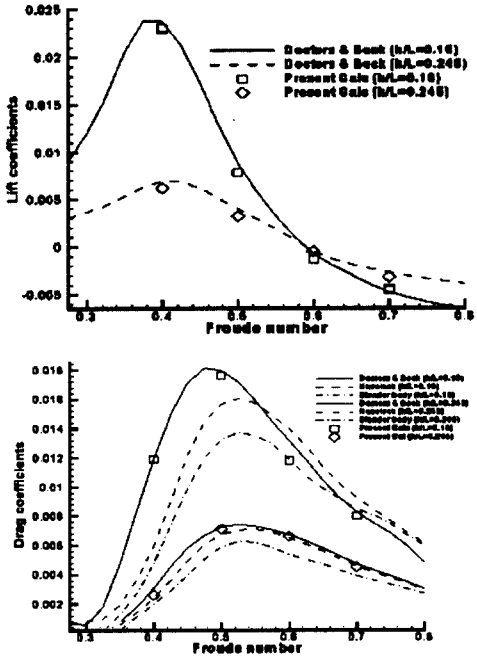

Fig. 4. Hydrodynamic coefficients at different Froude numbers.

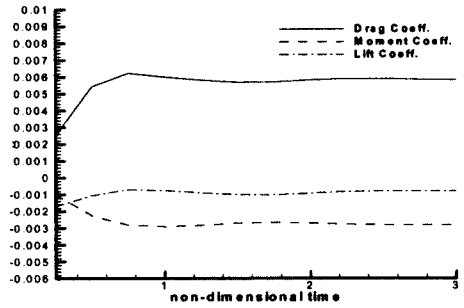

Fig. 5. Hydrodynamic coefficients along the time marching

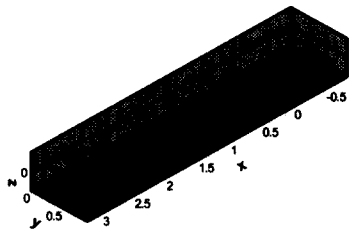

Fig. 6. Free surface wave simulation on center and side lines

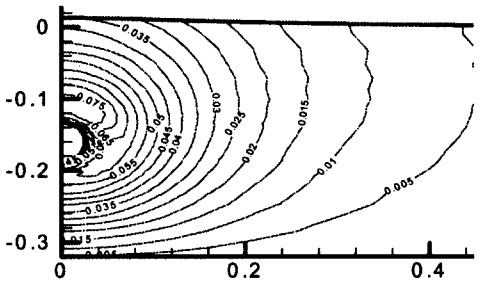

Fig. 7. Pressure contours around underwater vehicle(non-dimensionalized by $0.5\rho U^{2)}$)

results agree well with Doctors and Beck [6]. Fig. 5 shows the lift, drag and moment acting on the spheroid as a function of time. As seen, the solution is close to the steady state after the body has moved three body lengths. Fig. 6 shows the wave simulation on center and side lines. Fig. 7 shows the pressure contour around the underwater vehicle where the pressure is non-dimensionalized by 0.5 ρU^2.

Ⅳ. CONCLUSION

The flow characteristics for the underwater vehicle is numerically investigated by showing the wave patterns on the free surface. Hydrodynamic coefficients are compared at varying Froude numbers 0.4 to 0.7. The calculated results agree well with others' results. The lift, drag and moment are shown as a function of time. The

solution shows the steady state after the body has moved three body lengths.

REFERENCES

1) Ramaprian, B. R., Patel, V. C. and Choi, D. H. (1981). "Mean flow Measurements in the Three Dimensional Boundary Layer over a Body of Revolution at Incidence", Jour. Fluid Mech., Vol. 103, pp. 479-504

2) Intermann, G. A. (1986). "Experimental Investigation of the location and Mechanism of Local Flow Separation on a 3 Caliber Tangent Ogive Cylinder at Moderate Angles of Attack", M.S. Thesis, Univ. of Florida, Gainesville, Florida

3) Vasta, V. N., Thomas J. L. and Wedan, B. W. (1989), "Navier-Stokes Computations of Prolate at Angle of Attack", AIAA Jour., Vol. 26, No. 11, pp. 986-993

4) Hartwich, P. M., Hall, R. M. (1990), "Navier-Stokes Solution for Vortical Flow over a Tangent-Ogive Cylinder", AIAA Jour., Vol. 28, No. 7, pp. 1171-1179

5) Baldwin, B., Lomax, H. (1978), "Thin Layer Approximation and Algebraic Model for Separated Turbulent Flows", AIAA paper, No. 78-257

6) Doctors, L. J., Beck, R. F. (1987), "Convergence properties of the Neumann-Kelvin problem for a Submerged Body", J. Ship Research, 31, pp. 227-234